Microarray analysis of fiber cell maturation in the lens

Dmitry Ivanov[a,b], Galina Dvoriantchikova[a], Anna Pestova[a,b], Lubov Nathanson[c], Valery I. Shestopalov[a,d,*]

[a] *Bascom Palmer Eye Institute, Department of Ophthalmology, University of Miami Miller School of Medicine, 1638 NW 10th Avenue, Miami, FL 33136, USA*
[b] *Vavilov Institute of General Genetics RAS, Moscow, Russia*
[c] *Department of Molecular and Cellular Pharmacology, University of Miami Miller School of Medicine, Miami, FL, USA*
[d] *Department of Cell Biology and Anatomy, University of Miami Miller School of Medicine, Miami, FL, USA*

Received 12 October 2004; revised 23 December 2004; accepted 7 January 2005

Available online 21 January 2005

Edited by Lukas Huber

Abstract The mammalian lens consists of an aged core of quiescent cells enveloped by layers of mature fully elongated cells and younger, continuously elongating transcriptionally active cells. The fiber cell maturation is initiated when fiber cells cease to elongate. The process of maturation represents a radical switch from active elongation to a life-long quiescence and has not been studied previously. It may also include critical stages of preparation for the organelle removal and denucleation. In the present study, we used laser capture microdisection (LCM) microdissection and RNA amplification to compare global gene expression profiles of young elongating and mature, non-elongating fiber cells. Analysis of microarray data from three independent dye-swap experiments identified 65 differentially expressed genes (FDR < 0.1) with greater than 2-fold change in expression levels. Microarray array results for a group of randomly selected genes were confirmed by quantitative RT-PCR. These microarray results provide clues to understanding the molecular pathways underlying lens development. The identified changes in the profile of gene expression reflected a shift in cell physiology characterizing the lens fiber maturation.

Keywords: Lens; Differentiation; Microarray; Gene expression profiling; Laser capture microdissection; RNA amplification

1. Introduction

The lens of the eye has become an important model system for studies of fundamental biological processes, such as cellular differentiation and aging. The lens tissue is composed of the tightly packed mass of fiber cells enveloped by a monolayer of epithelial cells on the anterior side. Lens fibers are ribbon-like cells that differentiate continuously from the lens epithelium throughout life [1]. This differentiation requires dramatic changes in shape, length, volume, protein content and removal of the organelle complement leading to an increase in transparency of the mature fibers in the core of the lens [2]. The differentiation of the lens fiber cells consists of two intense phases: first, the cells differentiate from the lens epithelium in order to begin elongation [3,4] and second, after elongation is accomplished the deeply buried fibers eliminate organelles and convert to quiescence [5]. More subtle changes occur between these intense phases, including fiber cell maturation, which coincides temporally with a true syncytium formation in the core of the lens [6,7]. The maturation phase represents a radical switch from active elongation to a life-long quiescence. Although this phase includes critical stages of cell preparation for the organelle removal and denucleation, accumulation of crystallins and cell fusion, it has not been previously explored. Investigations of the molecular events of the first differentiation event have been facilitated by the superficial location of the transforming cells and the availability of a lens epithelium cell culture model [8,9]. In contrast, studies of the second differentiation phase occurring in the deeper layers of the tissue are more challenging, in part due to the lack of an appropriate cell culture model [8–10]. These obstacles also complicate the use of microarray transcriptional profiling, which has been so far restricted to sampling the whole lenses [11,12] or epithelial cell explants [13–15] at different ages. Direct gene expression profiling of the deeper layers of the lens has been impossible for two main reasons: (1) lack of differentiation-specific in vivo labeling that would allow dividing a featureless mass of maturing fibers into fractions with distinct differentiation status and (2) lack of a precise microdissection technique. Such precise differentiation-specific partitioning has become possible only recently because of the generation of several novel GFP-expressing mouse models [16] and development of the LCM technique [17,18]. Lenses of TgN(GFPU)5Nagy mice possess "variegated" mosaic GFP labeling outside the syncytium, which allows the separation of "variegated" elongating cells from uniformly labeled maturing cells. Also, recent advances in linear RNA amplification methods [19,20] ensured reliable preparation of RNA probes from ultra-small samples generated by LCM. The combination of these technical innovations has made it possible to perform direct transcriptional profiling of LCM-dissected lens fibers [21,22].

In this work, we sought to compare global gene expression in fully elongated, maturing fiber cells in the syncytium, with younger, actively elongating cells derived from the region outside the syncytium borders. To identify molecular pathways associated with lens differentiation, we characterized changes

*Corresponding author. Fax: +1 305 547 3658.
E-mail address: vshestopalov@med.miami.edu (V.I. Shestopalov).

Abbreviations: LCM, laser capture microdisection

0014-5793/$30.00
doi:10.1016/j.febslet.2005.01.016

in gene expression by differential microarray profiling of these tightly spaced lens regions.

2. Materials and methods

2.1. Animals

Mice were housed in animal care facilities according to NIH guidelines (NIH Publication No. 86-23, 1985) and University of Miami IACUC approved protocols. All experiments were performed in compliance with the ARVO statement for use of animals in ophthalmic and vision research. The transgenic mouse strain used in this study TgN(GFPU)5Nagy (Jackson Laboratory, Bar Harbor, ME, originally generated in the laboratory of Andras Nagy [16]) express GFP ubiquitously and has no detectable lens abnormalities. Mouse lenses at P5 possess fiber cells at all stages of differentiation; in addition they are significantly easier to process for high quality microscopy and LCM samples then more aged ones. Animals were euthanized by CO_2 inhalation according to the IACUC approved protocol.

2.2. Tissue fixation and preparation

Lenses were removed and immediately fixed using 4% paraformaldehide/PBS or methanol-based UMFIX reagent (Sakura Finetek USA, Inc.). To map the exact location of both elongating and maturing fibers on the lens slices, 4% paraformaldehide/PBS fixed lenses were vibratome-sliced (Vibratome 1000, St. Louis, MO) as described previously [23] and the GFP expression pattern was captured by confocal microscopy. For RNA extraction, lens UMFIX-fixed tissue was sliced into 5 μm-thick paraffin sections and microdissected using LCM (Leica Microsystems, Bannockburn, IL). The mid-saggital slices were used both for syncytium border measurements and for LCM. Control measurements confirmed that similar rates of shrinkage in paraformaldehyde- and UMFIX-fixed samples did not affect the precision of LCM dissection (data not shown).

Fiber cell samples were dissected out of 5 μm-thick slices. In one experiment we typically processed about 40 slices pooled from P5 littermate lenses, which was sufficient to collect the minimum of 200 zone-specific cells. This sample size provided a reliable representation of RNA species in experimental procedures originally designed and tested for only 1–10 cells [21,22,24].

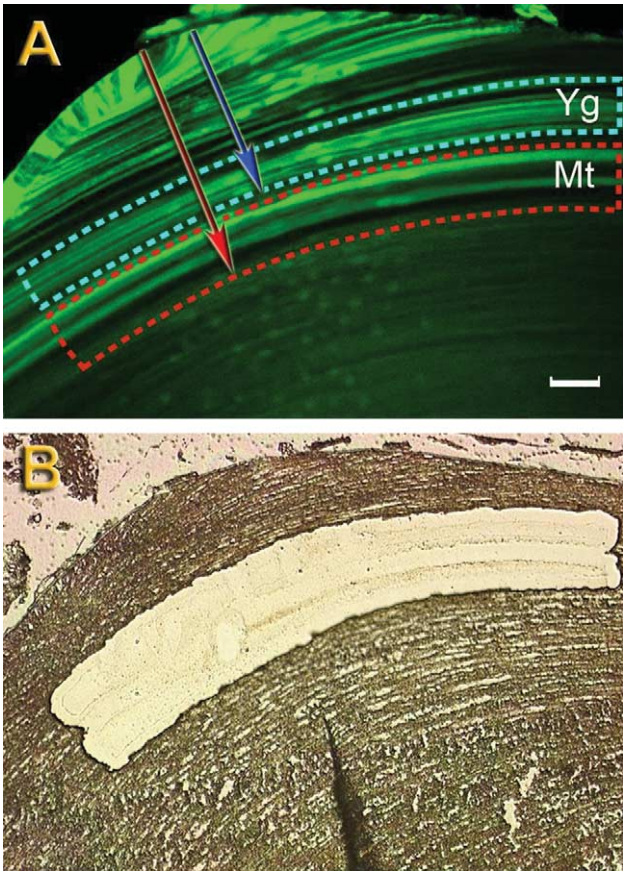

Fig. 1. Maturing and young fibers were discriminated in the TgN(GFPU5)Nagy mouse lenses using contrasting GFP labeling patterns (A). Mature fibers (Mt) were localized within the region of uniform GFP labeling, whereas young (Yg) fibers localized exclusively to the variegated region at the lens periphery. Paraffin sections of P5 lenses were microdissected by LCM using measurements performed on the contralateral eye (red and blue arrows correspond to the inner borders of the maturing and young fibers) (B). Cells cut from each of the two regions were collected. Bar is 50 mkm.

2.3. Microscopy

Lenses were fixed in 4% paraformaldehyde/PBS and sectioned with a vibratome as described previously [25]. Localization of the syncytium border defined by the abrupt change of GFP labeling pattern was captured by confocal microscopy as described previously [23]. In brief, GFP fluorescence was visualized using an LSM510 instrument (Carl Zeiss, NY) equipped with an argon laser at 488 nm excitation and a 515–565 nm band pass emission filter. Physical parameters of the zones containing young and maturing fibers were measured in fixed lens slices using the software provided by Zeiss (Fig. 1A).

2.4. Lens microdissection and RNA extraction

Cells from elongating and maturing fiber regions were dissected out using the Leica DMLA laser capture microscope (Leica Microsystems, Bannockburn, IL). The cut-out pieces containing captured cells were placed directly into tubes containing the lysis buffer supplied in the Absolutely RNA® nanoprep kit (Stratagene, La Jolla, CA) and total RNA was extracted and purified using the Absolutely RNA nanoprep kit according to the manufacturer's protocol. Caps briefly placed onto

Table 1
Primers used in RT-PCR analysis

Kpnb3	Forward	GTGAATGTGGAGGAGGTCT
	Reverse	TCAGTCCACAATCCTCCAG
Ivns1abp	Forward	GGCTCTGATCCATATGGTC
	Reverse	CATCAAAGCCACCACCTAC
Pfkfb3	Forward	TTGAATGTAGAATCGGTGAGC
	Reverse	CATCTCGGCTTTAGTGCTTC
Gadd45b	Forward	GGGGGATTTTGCAATCTTCT
	Reverse	CGGTGAGGCGATCCTGA
Srcasm	Forward	CGCCTCGAGTCACACATATG
	Reverse	TTTAGAGAGCTGGCCCTTTG
App	Forward	GACAAACATCAAGACGGAAG
	Reverse	TTCTGCTGCATCTTGGAGAG
Cd9	Forward	TGGAGCAGTGGGTATCGGCATC
	Reverse	TAAATTGAACCCCCGGATCCCTC
Stx11	Forward	GTTCGGGGTTGGCTGGAG
	Reverse	CTCTGCAAGCCGATCCTTC
Adam12	Forward	ATAGGCATTGTGGGAAGGTC
	Reverse	CCGTCCCACAGCTTCAGTC
Crybb3	Forward	GAGGCAGAAGTATCCCCAGA
	Reverse	GGAGGGACAGGAGAATGTCA
Actb	Forward	CACCCTGTGCTGCTCACC
	Reverse	GCACGATTTCCCTCTCAG

the section without laser activation were used as negative controls. Samples from several age-matched lenses were pooled together to obtain differentiation-specific samples for microarray analysis.

2.5. RT-PCR

The quality of the extracted RNA was determined by RT-PCR using primers for mouse β-actin and low copy genes (Table 1 and Fig. 2) and MessageSensor™ RT Kit (Ambion, USA). Following conditions were used for one step RT-PCR: initial reverse transcription for 30 min at 50 °C, followed by Taq activation at 95 °C for 15 min, followed by 40 cycles at 94 °C, 45 s; 58 °C, 45 s; 72 °C, 1 min; and hold for 5 min at 72 °C.

2.6. RNA amplification and labeling

Target RNA amplification and labeling with Cy-3 or Cy-5 dyes from CyDye Post-labeling Reactive Dye Pack (Amersham, USA) was carried out in two rounds using the Amino Allyl MessageAmp™ aRNA Kit (Ambion) as specified by the manufacturer. Quality and size distribution of the targets were determined by the Agilent 2100 Bioanalyzer (Agilent Technologies, USA). The Amino Allyl MessageAmp aRNA Kit is configured to incorporate the modified nucleotide 5-(3-aminoallyl)-UTP (aaUTP) into the aRNA during in vitro transcription. Once purified and fragmented, the dye labeled aRNA was used for microarray hybridization.

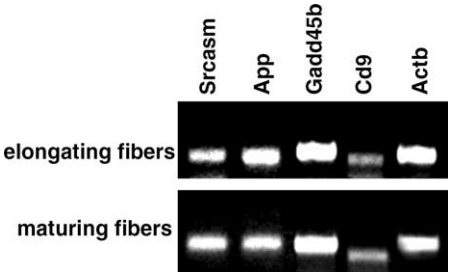

Fig. 2. The quality of the extracted RNA from elongating and maturing zones in the lens was determined by RT-PCR using primers for mouse *Actb* (β-actin), *Gadd45b*, *App*, *Cd9*, *Srcasm*.

2.7. Array hybridization

Labeled and amplified RNA from three different biological experiments were hybridized to the 22K Mouse Oligo microarrays (Agilent Technologies) according to the manufacturer's instructions. For each biological replicate we performed two technical subreplicates using a dye-swap.

2.8. Image analysis and data processing

The microarrays were scanned at 10 μm resolution using a GenePix 4000A scanner (Axon Instruments at Molecular Devices) and the resulting images were analyzed with the software package GenePix Pro 5.1 (Axon Instruments at Molecular Devices). Data extracted from the images were transferred to the software package Acuity 4.0 (Axon Instruments) for normalization and statistical analysis. Each array was normalized for signal intensities across the whole array and locally, using Lowess normalization. For further analysis genes were selected according to the following quality criteria: (1) at least 90% of the pixels in the spot had intensity higher than background plus two standard deviations; (2), there were less than 2% saturated pixels in the spot; (3) signal to noise ratio (defined as ratio of the background subtracted mean pixel intensity to standard deviation of background) was 3 or above for each channel; (4) the spot diameter was between 110 and 150 μm; (5) the regression coefficient of ratios of pixel intensity was 0.6 or above. To identify significantly expressed genes we used one-class SAM (Significant Analysis of Microarray, http://www-stat.stanford.edu/~tibs/SAM) [26] analysis and NIA Array Analysis ANOVA (http://lgsun.grc.nia.nih.gov/ANOVA) tool. The following criteria were used: with SAM the FDR (False Discovery Rate) was less than 0.5% and the average fold change was greater than 2.0; for NIA ANOVA the FDR was less than 10%, Bayesian adjustment of error variance was implemented and mean error variance was calculated using a sliding window of 1000 probes. NIA ANOVA software performs calculation of the FDR values for individual genes; these values are included into Tables 2 and 3. All primary microarray data are available at the GEO web site (http://www.ncbi.nih.gov/geo/; series GSE2083). Selected genes were classified according to Gene Ontology category "biological process" using Onto-Express (http://vortex.cs.wayne.edu/Projects.html) [27,28].

2.9. Verification of microarray data

The microarray gene expression data were verified by quantitative RT-PCR for a group of randomly selected genes (Tables 1 and 4). cDNA was synthesized using the Message Sensor™ RT Kit and real-time RT-PCR was performed with gene specific primers using

Table 2
Genes with elevated expression in the maturing fibers

GenBank Accession Number	Gene product	Expression ratio	FDR (ANOVA)	Biological process
				Signal transduction
AK034430	Latrophilin 2 (*Lphn2*)	2.46	0.00378	
NM_172615	RIKEN cDNA 1700021K19 gene (*1700021K19Rik*)	2.21	0.02717	
NM_008715	DEAD/H (Asp-Glu-Ala-Asp/His) box polypeptide 26 (*Ddx26*)	2.29	0.00284	
				Cytoskeleton organization and biogenesis
NM_023668	Nuclear distribution gene E-like homolog 1 (*Ndel1*)	2.09	0.03422	
AK077135	Myosin 18B (*Myo18B*)	2.22	0.00032	
				Apoptosis
NM_008655	Growth arrest and DNA-damage-inducible 45 β (*Gadd45b*)	3.90	0	
NM_013863	Bcl2-associated athanogene 3 (*Bag3*)	2.33	0.00304	
NM_019957	Deoxyribonuclease II β (*Dnase2b*/*Dlad*)	2.85	0.00027	
				Endocytosis and exocitosis
NM_028733	Protein kinase C and casein kinase substrate in neurons 3 (*Pacsin3*)	2.05	0.04356	
AK017897	Syntaxin 11 (*Stx11*)	4.75	0	
				Metabolism
NM_145835	Lactase-like (*Lctl*)	2.30	0.00235	
				Unknown
AK032259	RIKEN cDNA 3110001E11 gene (*3110001E11Rik*)	2.95	0	
NM_172275	FLN29 gene product (Fln29-pending)	2.05	0.02598	
NM_172641	RIKEN cDNA 9930023K05 gene (*9930023K05Rik*)	2.45	0.00193	

Table 3
Genes with lowered expression in the maturing fibers

GenBank Accession Number	Gene product	Expression ratio	FDR (ANOVA)	Biological process
				Signal transduction
NM_009790	Calmodulin 1 (*Calm1*)	−2.07	0.0478	
NM_009861	Cell division cycle 42 homolog (*S. cerevisiae*) (*Cdc42*)	−2.16	0.08763	
NM_008760	Osteoglycin (*Ogn*)	−2.24	0.00242	
NM_010696	Lymphocyte cytosolic protein 2 (*Lcp2*)	−2.45	0.02637	
NM_054102	Influenza virus NS1A binding protein (*Ivns1abp*)	−2.51	0.00029	
NM_025618	Sorcin (*Sri*)	−2.83	0.01369	
NM_011239	RAN binding protein 1 (*Ranbp1*)	−2.01	0.0193	
				Cytoskeleton organization and biogenesis
NM_146243	ARP2 actin-related protein 2 homolog (yeast) (*Actr2*)	−2.03	0.03162	
NM_009510	Villin 2 (*Vil2*)	−2.26	0.00538	
NM_008538	Myristoylated alanine rich protein kinase C substrate (*Marcks*)	−2.12	0.00818	
NM_138744	Synovial sarcoma, X breakpoint 2 interacting protein (*Ssx2ip*)	−2.29	0.00541	
				Development and cell differentiation
NM_010825	Myeloid ecotropic viral integration site-related gene 1 (*Mrg1*/*Meis2*)	−2.29	0.00539	
NM_008885	Peripheral myelin protein (*Pmp22*)	−2.36	0.03025	
NM_011857	Odd Oz/10-m homolog 3 (*Drosophila*) (*Odz3*)	−2.15	0.003	
NM_021881	Quaking (*Qk*)	−2.02	0.02641	
				Cell cycle
NM_019914	ALL1-fused gene from chromosome 1q (*Af1q-pending*)	−2.11	0.01548	
NM_146207	Cullin 4A (*Cul4a*)	−2.65	0.00173	
NM_015781	Nucleosome assembly protein 1-like 1 (*Nap1l1*)	−2.82	0.00025	
				Transport
NM_178405	ATPase, Na+/K+ transporting, α2 polypeptide (*Atp1a2*)	−2.08	0.00891	
NM_023579	Karyopherin (importin) β3 (*Kpnb3*)	−2.83	0	
NM_020573	Oxysterol binding protein-like 1A (*Osbpl1a*)	−2.10	0.0134	
AK083630	Src activating and signaling molecule (*Srcasm*)	−3.55	0	
NM_009037	Reticulocalbin (*Rcn*)	−2.50	0.0005	
NM_013703	Very low density lipoprotein receptor (*Vldlr*)	−2.10	0.03991	
NM_013898	Translocase of inner mitochondrial membrane 8 homolog a (yeast) (*Timm8a*)	−2.23	0.01784	
				Cell adhesion
NM_007664	Cadherin 2 (*Cdh2*)	−3.74	0	
BC034120	Vitrin (Vit)	−2.08	0.00981	
				ECM
NM_009984	Cathepsin L (*Ctsl*)	−2.79	0.00029	
J04694	Procollagen, type IV, α1 (*Col4a1*)	−2.12	0.06809	
				Regulation of transcription
NM_026003	SWI/SNF related, matrix associated, actin dependent regulator of chromatin, subfamily a, member 2 (*Smarca2*)	−3.95	0	
BC043450	Zinc finger protein 198 (*Zfp198*)	−2.53	0.00053	
NM_024186	Single-stranded DNA binding protein 2 (*Ssbp2*)	−2.07	0.03019	
				Metabolism
NM_145942	3-Hydroxy-3-methylglutaryl-coenzyme A synthase 1 (*Hmgcs1*)	−2.34	0.0361	
NM_019868	Heterogeneous nuclear ribonucleoprotein H2 (*Hnrph2*)	−2.10	0.07653	
NM_133232	6-Phosphofructo-2-kinase/fructose-2,6-biphosphatase 3 (*Pfkfb3*)	−2.42	0.00097	
NM_007933	Enolase 3, β muscle (*Eno3*)	−2.19	0.01283	
NM_145360	Isopentenyl-diphosphate δ isomerase (*Idi1*)	−2.55	0.00033	
NM_025573	Splicing factor, arginine/serine rich 9 (*Sfrs9*)	−2.09	0.00778	
NM_053188	Steroid 5α-reductase 2 (*Srd5a2*)	−3.32	0.00274	
				Unknown
NM_012056	FK506 binding protein 9 (*Fkbp9*)	−2.59	0.00778	
NM_026618	DNA segment, Chr 11, ERATO Doi 99, expressed (*D11Ertd99e*)	−2.05	0.04342	
NM_053194	Expressed sequence AI114950 (*AI114950*)	−2.71	0.00887	
AK029831	RIKEN cDNA 6620401M08 gene (*6620401M08Rik*)	−2.86	0.0009	
AK011900	RIKEN cDNA 2610206D03 gene (*2610206D03Rik*)	−2.36	0.00928	
NM_144846	RIKEN cDNA 0910001A06 gene (*0910001A06Rik*)	−2.04	0.018	
NM_016809	RNA binding motif protein 3 (*Rbm3*)	−2.62	0.00016	
AA755091	RIKEN cDNA 1190005I06 gene (*1190005I06Rik*)	−2.06	0.01361	
NM_023215	RIKEN cDNA 2500003M10 gene (*2500003M10Rik*)	−2.10	0.00407	
NM_172779	RIKEN cDNA 6330505F04 gene (*6330505F04Rik*)	−2.55	0.00035	
AK048051	RIKEN cDNA 1810011E08 gene (*1810011E08Rik*)	−2.25	0.01065	
BC008232	Mus musculus, clone IMAGE:2647796, mRNA	−2.41	0.00105	

Note: "minus" sign in expression ratio column is used solely to indicate the decrease in expression level.

Table 4
Validation of microarray data for randomly selected genes by quantitative RT-PCR

	Real time RT-PCR (expression ratio)	Array (expression ratio)	Confirmed by real-time PCR
Kpnb3	−3.5	−2.83	Yes
Ivns1abp	−2.4	−2.51	Yes
Pfkfb3	−10.4	−2.42	Yes
Srcasm	−5.1	−3.55	Yes
Gadd45b	2.6	3.90	Yes
Stx11	2.2	4.75	Yes
Adam12[a]	1.2	1.14	Yes
Crybb3[a]	1.0	1.22	Yes
Cd9[b]	3.0	5.56	Yes

[a]Two genes with less then 2-fold change were tested for the false negative signals.
[b]The gene with more then 2-fold change in expression detected in two out of three experiments.
Note: "minus" sign in expression ratio column is used solely to indicate the decrease in expression level.

the QuantiTect SYBR Green PCR kit (Qiagen, Valencia, CA) on a Bio-Rad I-Cycler. The PCR conditions were as follows: 95 °C, 15 min; 45 cycles at 94 °C, 30 s; 58 °C, 30 s; 72 °C, 1 min. The measured transcript abundance was normalized to the level of *Actb* (β-actin) for all samples. The size of the amplified PCR product was confirmed by gel electrophoresis.

3. Results and discussion

To characterize changes associated with the shift from elongation to maturation that precede organelle loss in lens fiber cells, we used the TgN(GFPU)5Nagy mouse strain to permit differentiation-specific staging of lens fiber cells in vivo. This strain exhibits a mosaic GFP expression pattern in many tissues, including lens, most likely due to position effect variegation phenomenon [23]. The lenses of TgN(GFPU)5Nagy mice exhibit contrasting GFP labeling patterns in young, superficial fibers, compared with older, maturing fibers: a superficial layer of young cells retains the mosaic (variegated) GFP expression pattern while the maturing fibers become uniformly fluorescent (Fig. 1A). As shown previously, an abrupt change from mosaic into the uniformly labeled fiber mass occurs when cells reach a specific differentiation stage and connect to the core syncytium [23]. At this stage elongation is accomplished and maturation begins. In this work we used the well-defined border of the syncytium as a marker separating young elongating fiber cells from a cohort of cells in which the maturation process leading to organelle degradation and quiescence has been initiated. Microscopic visualization allowed us to microdissect zones containing sub-populations of elongating and maturing fibers, enabling us to characterize the gene expression profile of cell at a discrete stage of differentiation.

We microdissected young and maturing fibers as follows: (1) young fibers containing only variegated fibers located outside (at least 30 μm or six cell layers away from the border) of the uniformly labeled syncytium; (2) maturing fibers containing uniformly labeled (syncytial) fibers located internally to the young ones (Fig. 1A). We reasoned that variegated fibers from the border of the syncytium should be included into "maturing fiber" sample in order to detect potential early transcription of genes responsible for fiber maturation and syncytium formation. Therefore, in a typical experiment we shifted borders of the dissected zones six cell layers or 30 μm (approximately one "differentiation day" of the mouse lens) closer to the lens surface (Fig. 1A). We used LCM, a technology capable of precise, RNA-safe microdissection at a single-cell resolution to prepare samples of the fixed tissue and extract high quality RNA for amplification and labeling. A minimum gap of 10 μm was used between the two dissected regions to avoid overlap and contamination between the subpopulations of sampled cells. One lens from each animal was used for LCM microdissection and RNA extraction; the lens from the contralateral eye was used to define the position of the GFP border by microscopy (Fig. 1A and B).

The high quality mRNA extracted from LCM microdissected lens tissue ensured successful amplification, labeling and reproducibility of microarray profiles. Linear RNA amplification of the samples used a T7-RNA polymerase-based technique, which is widely used for labeling of the low-yield RNA samples recently [19,20]. Despite concerns raised about possible alteration in the original transcript abundance during the amplification steps, recent studies showed that the ratios of gene expression levels in similarly amplified samples remained intact [29–31]. The results of qPCR verification of our microarray data fully support these conclusions and thus assessment of differential gene expression using RNA amplification can be performed with a high degree of confidence. Microarray data from three independent biological experiments were analyzed using the NIA ANOVA tool and SAM software to determine significantly differentially expressed genes. Genes that met the criteria (see Section 2) set for both methods and showed expression differences exceeding 2-fold are presented in Tables 2 and 3. We found that 65 genes were differentially expressed in excess of 2-fold in the maturing fibers cells compared with young elongating fibers. About 25% of genes were activated in maturing fibers; 75% were downregulated. Differential expression was verified for a group of randomly selected genes using quantitative RT-PCR (Table 4).

The differentiation of lens fiber cells involves extensive metabolic, morphologic and functional changes [32]. Because the lens is an avascular tissue, metabolic activity gradually decreases in fibers that became buried inside the tissue and lose direct exposure to the nutritious ocular humors. These gradual changes should be reflected as differences between the two transcriptional profiles we obtained in this study. Indeed, the expression of many genes encoding metabolic enzymes was decreased in the buried, maturing fibers (Table 3).

In contrast to gradual changes in metabolism-related genes, fiber maturation implies turning on a specific group of pathways for cell remodeling. It is now widely appreciated that fiber cell differentiation utilizes components of the apoptotic machinery (including caspases 3, 6 and 8) while controlling the extent of apoptosis with anti-apoptotic proteins [33–37]. Despite a well-documented activity of apoptotic proteases in the developing lens [4,5], transcriptional activation of the corresponding genes is not necessarily correlated with cell differentiation in time (Bassnett, personal communication). This discrepancy can be explained by the fact that major apoptotic "effector" proteases are activated post-translationally via enzymatic cleavage of inactive pro-proteins rather then at the transcriptional level [38,39]. The microarray analysis revealed several classes of apoptosis-related genes that were activated transcriptionally during fiber maturation (Table 2). For example, expression of *Gadd45b*, the upstream activator of p38 in

the TGFβ-induced apoptotic pathway [40], was activated (3.9-fold) in maturing fibers. Additionally, *Dlad* expression was elevated 2.85-fold in maturing fibers, reflecting transcriptional activation of this pathway prior to the start of organelle loss. *DLAD* (DNase II-like acid DNase, also called DNase IIbeta) is responsible for the degradation of nuclear DNA in apoptosis and during lens cell differentiation [5,34]; alteration of this process causes nuclear cataract [41,42]. Further, expression of the co-chaperone transcript *Bag3* was elevated in the maturing fibers. Bag3 participates in apoptosis regulation by interacting with several apoptosis-modulating factors. *Bag3* overexpression has been shown to inhibit apoptosis induced via Bax or Fas pathways in the HeLa cell line [43] and by IL-3 deprivation in the murine hematopoietic cell line 32D [44]. At the same time, *BAG3* downregulation enhanced the apoptotic response to chemotherapy in human primary B chronic lymphocytic leukemia cells [45]. Our data confirm previous reports that the balance of specific pro- and anti-apoptotic signals modulates lens fiber maturation and identifies potential mediators of apoptosis in the developing lens.

During lens fiber maturation, the protein-permeable intercellular communication pathway is initiated, leading to the formation of a true syncytium in the lens core [6,7]. This developmentally regulated pathway is likely facilitated by cell–cell fusions. [6]. Cell–cell fusions, which utilize molecular machinery distinct from the SNARE-regulated fusion of vesicles, are the focus of numerous studies as they are also intimately involved in forming developmental syncytia in gametes, osteoclasts, macrophages, placenta trophoblasts and skeletal muscle [46]. We examined our data for the evidence of transcriptional activation of previously identified as well as potential fusogenic proteins that may be implicated in lens syncytium formation. Unexpectedly, our data did not show transcriptional activation of the potentially "fusogenic" genes *ITGNB1*, *MFR*, *CD47* and *Adam12* in the maturing fibers. However, the *CD9* and *Pacsin3* both showed 2-fold increased expression (Tables 2 and 4). CD9 has been demonstrated to play a critical role in regulating myoblast and gamete fusion [47,48] and Pacsin3 is known to bind and activate potentially fusogenic Adam12, implicated in fusion of myoblasts and osteoclasts [49]. These data suggest that a CD9-mediated fusion pathway is active in the lens and that Adam12 activity may also be involved in this process via Pacsin3 but that it may be regulated at the post-translational level.

An intriguing feature of maturing lens fibers is the large upregulation of the *Stx11* gene (4.75-fold), a member of the SNARE family. SNAREs are small coiled-coil proteins required for specific membrane fusion events and are associated with secretory and endocytic pathways in eukaryotic cells [50]. Despite their previous implication only in vesicle fusion, a recent study raised the theoretical possibility that *Stx11* facilitates plasma membrane fusion [51]. Alternatively, maturing fibers might activate *Stx11*-mediated secretory pathways upon physical disconnection from the awashing ocular humors at the end of the elongation phase. In conclusion, the described changes in the gene expression profiles in this study reflected a shift in cell physiology, characteristic of the beginning of fiber maturation process. Our analysis suggests that genes previously shown to be implicated cell fusion are likely to be regulated post-translationally in the lens and have identified potentially novel players in syncytium-forming pathways. Future work will define the role of these genes in the developing lens.

Acknowledgments: We thank Dr. Vladimir Vincek for his expert technical assistance and the gift of the UM FIX solution, Dr. Chia-Yang Liu for expert advice in histology preparations, Dr. Abigail Hackam for the help with the manuscript preparation and the staff of the DNA Microarray Core Facility University of Miami for high quality microarray hybridizations and data preparation. This study was supported by NIH Grants *R01-EY14232* (V.S.), a Research to Prevent Blindness (RPB) Career Development Award (V.S.), an unrestricted Grant to the Department of Ophthalmology from RPB and an unrestricted Grant P30-EY014801 to the Bascom Palmer Eye Institute.

References

[1] Bhat, S.P. (2001) The ocular lens epithelium. Biosci. Rep. 21, 537–600, Review.
[2] Piatigorsky, J. (1981) Lens differentiation in vertebrates. A review of cellular and molecular features. Differentiation 19, 134–187, Review.
[3] Beebe, D.C., Compart, P.J., Johnson, M.C., Feagans, D.E. and Feinberg, R.N. (1982) The mechanism of cell elongation during lens fiber cell differentiation. Dev. Biol. 92, 54–63.
[4] Bassnett, S. and Beebe, D.C. (1992) Coincident loss of mitochondria and nuclei during lens fiber cell differentiation. Dev. Dyn. 194, 85–93.
[5] Bassnett, S. (2002) Lens organelle degradation. Exp. Eye Res. 74, 1–6, Review.
[6] Shestopalov, V.I. and Bassnett, S. (2000) Expression of autofluorescent proteins reveals a novel protein permeable pathway between cells in the lens core. J. Cell Sci. 113, 1913–1934.
[7] Shestopalov, V.I. and Bassnett, S. (2003) Development of a macromolecular diffusion pathway in the lens. J. Cell Sci. 116, 4191–4200.
[8] Bassnett, S. and Beebe, D.C. (1990) Localization of insulin-like growth factor-1 binding sites in the embryonic chicken eye. Invest. Ophthalmol. Vis. Sci. 31, 1637–1680.
[9] Beebe, D.C., Parmelee, J.T. and Belcher, K.S. (1990) Volume regulation in lens epithelial cells and differentiating lens fiber cells. J. Cell. Physiol. 143, 455–464.
[10] Shestopalov, V.I. and Bassnett, S. (2000) Three-dimensional organization of primary lens fiber cells. Invest. Ophthalmol. Vis. Sci. 41, 859–922.
[11] Mansergh, F.C., Wride, M.A., Walker, V.E., Adams, S., Hunter, S.M. and Evans, M.J. (2004) Gene expression changes during cataract progression in Sparc null mice: differential regulation of mouse globins in the lens. Mol. Vis. 10, 490–511.
[12] Wride, M.A., Mansergh, F.C., Adams, S., Everitt, R., Minnema, S.E., Rancourt, D.E. and Evans, M.J. (2003) Expression profiling and gene discovery in the mouse lens. Mol. Vis. 9, 360–396.
[13] Segev, F., Mor, O., Segev, A., Belkin, M. and Assia, E.I. (2005) Downregulation of gene expression in the ageing lens: a possible contributory factor in senile cataract. Eye 19, 80–85.
[14] Hawse, J.R., Hejtmancik, J.F., Huang, Q., Sheets, N.L., Hosack, D.A., Lempicki, R.A., Horwitz, J. and Kantorow, M. (2003) Identification and functional clustering of global gene expression differences between human age-related cataract and clear lenses. Mol. Vis. 9, 515–552.
[15] Ruotolo, R., Grassi, F., Percudani, R., Rivetti, C., Martorana, D., Maraini, G. and Ottonello, S. (2003) Gene expression profiling in human age-related nuclear cataract. Mol. Vis. 9, 538–586.
[16] Hadjantonakis, A.K., Gertsenstein, M., Ikawa, M., Okabe, M. and Nagy, A. (1998) Generating green fluorescent mice by germline transmission of green fluorescent ES cells. Mech. Dev. 76, 79–90.
[17] Todd, R., Lingen, M.W. and Kuo, W.P. (2002) Gene expression profiling using laser capture microdissection. Expert. Rev. Mol. Diagn. 2, 497–507, Review.
[18] Eltoum, I.A., Siegal, G.P. and Frost, A.R. (2002) Microdissection of histologic sections: past, present, and future. Adv. Anat. Pathol. 9, 316–338, Review.

[19] Van Gelder, R.N., von Zastrow, M.E., Yool, A., Dement, W.C., Barchas, J.D. and Eberwine, J.H. (1990) Amplified RNA synthesized from limited quantities of heterogeneous cDNA. Proc. Natl. Acad. Sci. USA 87, 1663–1670.
[20] Carter, M.G., Hamatani, T., Sharov, A.A., Carmack, C.E., Qian, Y., Aiba, K., Ko, N.T., Dudekula, D.B., Brzoska, P.M., Hwang, S.S. and Ko, M.S. (2003) In situ-synthesized novel microarray optimized for mouse stem cell and early developmental expression profiling. Genome Res. 13, 1011–1032.
[21] Kamme, F., Zhu, J., Luo, L., Yu, J., Tran, D.T., Meurers, B., Bittner, A., Westlund, K., Carlton, S. and Wan, J. (2004) Single-cell laser-capture microdissection and RNA amplification. Methods Mol. Med. 99, 215–238.
[22] Kelz, M.B., Dent, G.W., Therianos, S., Marciano, P.G., McIntosh, T.K., Coleman, P.D. and Eberwine, J.H. (2002) Single-cell antisense RNA amplification and microarray analysis as a tool for studying neurological degeneration and restoration. Sci. Aging Knowledge Environ. 9, Review.
[23] Shestopalov, V.I., Missey, H. and Bassnett, S. (2002) Delivery of genes and fluorescent dyes into cells of the intact lens by particle bombardment. Exp. Eye Res. 74, 639–688.
[24] Kamme, F., Salunga, R., Yu, J., Tran, D.T., Zhu, J., Luo, L., Bittner, A., Guo, H.Q., Miller, N., Wan, J. and Erlander, M. (2003) Single-cell microarray analysis in hippocampus CA1: demonstration and validation of cellular heterogeneity. J. Neurosci. 23, 3607–3622.
[25] Shestopalov, V.I. and Bassnett, S. (1999) Exogenous gene expression and protein targeting in lens fiber cells. Invest. Ophthalmol. Vis. Sci. 40, 1435–1478.
[26] Tusher, V.G., Tibshirani, R. and Chu, G. (2001) Significance analysis of microarrays applied to the ionizing radiation response. Proc. Natl. Acad. Sci. USA 98, 5116–5137.
[27] Khatri, P., Draghici, S., Ostermeier, G.C. and Krawetz, S.A. (2002) Profiling gene expression using onto-express. Genomics 79, 266–336.
[28] Draghici, S., Khatri, P., Martins, R.P., Ostermeier, G.C. and Krawetz, S.A. (2003) Global functional profiling of gene expression. Genomics 81, 98–104.
[29] Baugh, L.R., Hill, A.A., Brown, E.L. and Hunter, C.P. (2001) Quantitative analysis of mRNA amplification by in vitro transcription. Nucleic Acids Res. 29, e29.
[30] Pabon, C., Modrusan, Z., Ruvolo, M.V., Coleman, I.M., Daniel, S., Yue, H. and Arnold Jr., L.J. (2001) Optimized T7 amplification system for microarray analysis. Biotechniques 31, 874–879.
[31] Poirier, G.M.-C. and Erlander, M.G. (1998) Postdifferential display: parallel processing of candidates using small amounts of RNA. Methods 16, 444–452.
[32] Bassnett, S. and Beebe, D.C. (2004) in: Development of the Ocular Lens Lovicu (Lovicu, F.J. and Robinson, M.L., Eds.), Cambridge University Press, Cambridge, UK.
[33] Bassnett, S. (1997) Fiber cell denucleation in the primate lens. Invest. Ophthalmol. Vis. Sci. 38, 1678–1765.
[34] Bassnett, S. and Mataic, D. (1997) Chromatin degradation in differentiating fiber cells of the eye lens. J. Cell Biol. 137, 37–49.
[35] Dahm, R., Gribbon, C., Quinlan, R.A. and Prescott, A.R. (1998) Changes in the nucleolar and coiled body compartments precede lamina and chromatin reorganization during fibre cell denucleation in the bovine lens. Eur. J. Cell Biol. 75, 237–283.
[36] Dahm, R. (1999) Lens fibre cell differentiation – a link with apoptosis?. Ophthalmic Res. 31, 163–246, Review.
[37] Wride, M.A., Parker, E. and Sanders, E.J. (1999) Members of the bcl-2 and caspase families regulate nuclear degeneration during chick lens fibre differentiation. Dev. Biol. 213, 142–198.
[38] Shi, Y. (2004) Caspase activation: revisiting the induced proximity model. Cell 117, 855–863, Review.
[39] Danial, N.N. and Korsmeyer, S.J. (2004) Cell death: critical control points. Cell 116, 205–224, Review.
[40] Yoo, J., Ghiassi, M., Jirmanova, L., Balliet, A.G., Hoffman, B., Fornace Jr., A.J., Liebermann, D.A., Bottinger, E.P. and Roberts, A.B. (2003) Transforming growth factor-beta-induced apoptosis is mediated by Smad-dependent expression of GADD45b through p38 activation. J. Biol. Chem. 278, 43001–43008.
[41] Evans, C.J. and Aguilera, R.J. (2003) DNase II: genes, enzymes and function. Gene 322, 1–15, Review.
[42] Nishimoto, S., Kawane, K., Watanabe-Fukunaga, R., Fukuyama, H., Ohsawa, Y., Uchiyama, Y., Hashida, N., Ohguro, N., Tano, Y., Morimoto, T., Fukuda, Y. and Nagata, S. (2003) Nuclear cataract caused by a lack of DNA degradation in the mouse eye lens. Nature 424, 1071–1075.
[43] Lee, J.-H., Takahashi, T., Yasuhara, N., Inazawa, J., Kamada, S. and Tsujimoto, Y. (1999) Bis, a Bcl-2-binding protein that synergizes with Bcl-2 in preventing cell death. Oncogene 18, 6183–6190.
[44] Antoku, K., Maser, R.S., Scully Jr., W.J., Delach, S.M. and Johnson, D.E. (2001) Isolation of Bcl-2 binding proteins that exhibit homology with BAG-1 and suppressor of death domains protein. Biochem. Biophys. Res. Commun. 286, 1003–1010.
[45] Romano, M.F., Festa, M., Pagliuca, G., Lerose, R., Bisogni, R. and Chiurazzi, F. (2003) BAG3 protein controls B-chronic lymphocytic leukaemia cell apoptosis. Cell Death Differ. 10, 383–385.
[46] Jahn, R., Lang, T. and Sudhof, T.C. (2003) Membrane fusion. Cell 112, 519–542, Review.
[47] Kaji, K., Oda, S., Miyazaki, S. and Kudo, A. (2002) Infertility of CD9-deficient mouse eggs is reversed by mouse CD9, human CD9, or mouse CD81; polyadenylated mRNA injection developed for molecular analysis of sperm-egg fusion. Dev. Biol. 247, 327–361.
[48] Tachibana, I. and Hemler, M.E. (1999) Role of transmembrane 4 superfamily (TM4SF) proteins CD9 and CD81 in muscle cell fusion and myotube maintenance. J. Cell Biol. 146, 893–904.
[49] Mori, S., Tanaka, M., Nanba, D., Nishiwaki, E., Ishiguro, H., Higashiyama, S. and Matsuura, N. (2003) PACSIN3 binds ADAM12/meltrin alpha and up-regulates ectodomain shedding of heparin-binding epidermal growth factor-like growth factor. J. Biol. Chem. 278, 46029–46063.
[50] Ungar, D. and Hughson, F.M. (2003) SNARE protein structure and function. Annu. Rev. Cell Dev. Biol. 19, 493–517, Review.
[51] Hu, C., Ahmed, M., Melia, T.J., Sollner, T.H., Mayer, T. and Rothman, J.E. (2003) Fusion of cells by flipped SNAREs. Science 300, 1745–1754.